RESEARCH PAPER | Physics of Materials | Volume : 4 | Issue : 11 | November 2014 | ISSN - 2249-555X

C70 Cleavable Steel and Powder Metal Forged Analytical and Numerical Study of the Elastic Thermo Mechanical Behavior Connecting Rod of the Four-Stroke Diesel Engine

KEYWORDS: connecting rod, powder metal forged and C70 Steel, Cast3m, Mathematica, stress, strain.

A. Soufi	A. Bakali	M. Talea
Labo de Physique de la Matière Condensée et Matériaux, Faculté des Sciences Ben M'sik	Labo de Physique de la Matière Condensée et Matériaux, Faculté des Sciences Ben M'sik	Labo de Physique de la Matière Condensée et Matériaux, Faculté des Sciences Ben M'sik

B. Boubeker	J.Grilhé	M. Mansouri
Labo de Physique de la Matière Condensée et Matériaux, Faculté des Sciences Ben M'sik	Institut P', Université de Poitiers, ENSMA, SP2MI- Téléport 2, F86962 Futuroscope-Chasseneuil cedex, France	Ecole Nationale des Sciences Appliquées, Khouribga. Université Hassan 1er Settat

ABSTRACT *Today, engine failures are rare but they are always possible despite the high engine reliability. These failures can result from a defect in cooling, a storage problem or maintenance. Premature wear of a mechanical part and sometimes bad conditions of use of the driver the engines are not always immune to failure (ignition, power, defaulters accessories such as connecting rod, crankshaft etc ... pieces that form the central part of the mechanics of the engine, and are normally solicited by various thermomechanical efforts (stress, compression, bending, expansion ...).*

In this context, we conducted an analytical and numerical Comparative study of resistance to thermo-mechanical fatigue concerning two connecting rods forged by the two most often used techniques in the world, namely the metal powder forged and forged steel C70.

The connecting rods are submitted to mechanical forces of compression pressure, and the effect of heat of combustion. The extraction of the stresses, strains and displacements using the computer code Castem based on finite element method allows us to classify materials according to the two most reliable

1- Introduction

The Powder Metallurgy was considered à lost art, it is as old as art potters and ceramicists. Unlike clay and other ceramic materials, the art of molding and firing metal objects or decorative practices were occasionally applied during the early phases of history. Metal sintering was completely forgotten over the following centuries, before being revived in Europe in the late 18th century, when various methods of producing platinum powder were observed (Table below).

Period	Developed technology	Country origin
1822	Platinum powder solid ingot	France
1830	sintering components of various metals	Europe
1915-1930	cemented carbide	Germany
1950 and 1960	Forged P / M and dispersion reinforced products, including P / M of forgings produced	United States
1990	intermetallic metal matrix composites, nano spray powders, and hot compacting	United States, England

What was that purely empirical ancestral techniques, turned into a scientific discipline in 1930, and following this challenge we have begun to understand the phenomena observed.

We notice that powder metallurgy has applications in several areas of engineering production of high volume pieces for the automotive industry (bearings, connecting rods, crankshaft, brakes, airbags, and other complex components ...), production of unrefined materials high performance, biomaterials, food additives, etc. ...

Today, the technology of powder metallurgy PM enables the production of steels with properties unattainable by conventional metallurgy from a process of atomization metal powders hot compacted.

Most connecting rods engine in the automotive sector are powder metal forged. These connecting rods are often subjected to deformation under the effect of «gas forces and mass forces".

Axial force causing an axial failure

Volume : 4 | Issue : 11 | November 2014 | ISSN - 2249-555X

Following the emergence of a new material "XC70 or C70 steel " cleavable in recent years, whose chemical composition comprises, by weight: 0.6% to 0.75% carbon addition to other additives "Mn , Cr, Mo etc. "Having good machinability, and can achieve brittle fracture in satisfactory industrial conditions, the data has changed in the automotive market, and this material is currently a competitor for powder metallurgy metal" MPM ".

In this work, we compare the behavior of both materials engineering precedents under the action of axial loads on connecting rod following:

- A kinematic study : piston and connecting rod system
- A dynamic study: determination of loads
- A thermodynamic study to determine the gas pressure
- A thermoelastic study (linear thermal expansion)
- A graphical study of loads according to the crank angle: The Mathematica software
- Numerical simulation the two connecting rods (PM and C70): the computer code used "CAST3M" to extract the fields of stresses, strains and corresponding displacements.

2- kinematic study

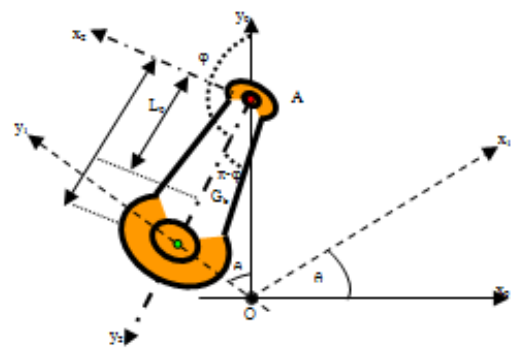

Operating Schemes

Kinematics of piston

Engine at full speed

$$\begin{cases}\delta = \dfrac{L_1}{r} = 4 \\ \omega = 209.44 rad/s = 2000 tr/\min\end{cases}$$

piston speed

$$\frac{v_p}{L_1} = \frac{-\dot{\theta}}{\delta}.\left(1+\frac{\cos\theta}{\delta}\right).\sin\theta = \frac{-209.44}{4}.\left(1+\frac{\cos\theta}{4}\right).\sin\theta$$

acceleration of piston

$$\frac{\gamma_p}{L_1} = \frac{d\left(\frac{v_p}{L_1}\right)}{dt} = \frac{-\dot{\theta}}{\delta}.\frac{d\left(1+\frac{\cos\theta}{\delta}\right).\sin\theta}{dt} = \frac{-\omega^2.\cos\theta}{\delta} - \frac{\omega^2.\cos 2\theta}{\delta^2} = \frac{\gamma_1}{L_1} + \frac{\gamma_2}{L_1}$$

Kinematics of the connecting rod

$$\overrightarrow{v_{G\in R_0}} = \begin{cases} \text{illegible} \\ -r.\dot{\theta}.\sin\theta + (L - L_0).\dot{\varphi}.\sin\varphi \\ 0 \end{cases}$$

$$\overrightarrow{\gamma_{G/R_0}} = \begin{cases} \dfrac{L_0.\dot{\theta}^2.\sin\theta}{\delta} \\ r.\dot{\theta}.\left(\varphi - \dfrac{L_0}{L_1}.\dot{\varphi} - \dot{\theta}\right).\cos\theta + r.\ddot{\varphi}.\left(1-\dfrac{L_0}{L_1}\right).\sin\theta \\ 0 \end{cases}$$

3- Dynamic study of the connecting rod and piston

$$\begin{cases} m_{bielle}.\dfrac{L_0}{\delta}.\dot{\theta}^2.\sin\theta = F_{Ax} + F_{Bx} \\ m_{bielle}.r.\dot{\theta}.\left[\varphi - \dot{\theta} - \dfrac{L_0}{L_1}.\dot{\varphi}\right].\cos\theta + m_{bielle}.r.\ddot{\varphi}.\left(1-\dfrac{L_0}{L_1}\right).\sin\theta = F_{Ay} + F_{By} - m_{bielle}.g \\ \kappa.\ddot{\varphi} = (L_0 - L_1).\left[F_{Bx}.\cos\varphi + F_{By}.\sin\varphi\right] + L_0.\left(F_{Ax}.\cos\varphi + F_{Ay}.\sin\varphi\right) \\ -F_{Ax} + F_{Hx} = 0 \\ m_{piston}.(r.\dot{\theta}.(\varphi - \dot{\theta}).\cos\theta + r.\ddot{\varphi}.\sin\theta) = -F_{Ay} - F_{Qy} - m_{piston}.g \end{cases}$$

$$F_{Qy} = S_{piston}.P(\theta) = \frac{\pi.D^2}{4}.P(\theta)$$

4- thermodynamic study.

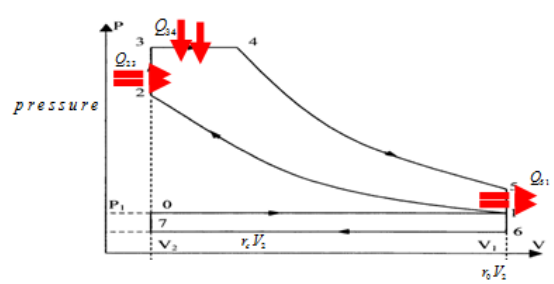

the mixed cycle

Intake	$P(\theta) \le 1.0135.10^5 Pa$	$0 \le \theta \le \pi$
Compression	$P(\theta) = \dfrac{P_0 V_0^{\gamma}}{\left(V_m + r(1-\cos\theta) + L_1\left(1-\sqrt{1-\frac{r^2\sin^2\theta}{L_1^2}}\right)\frac{\pi.D^2}{4}\right)^{\gamma}}$	$\pi \le \theta \le 2\pi$
Combustion	$P(\theta) = \dfrac{P_0 V_0^{\gamma}}{\left(V_m + r(1-\cos\theta) + L_1\left(1-\sqrt{1-\frac{r^2\sin^2\theta}{L_1^2}}\right)\frac{\pi.D^2}{4}\right)^{\gamma}}$	$2\pi \le \theta \le 3\pi$
Exhaust	$P(\theta) \ge 1.0135.10^5 Pa$	$3\pi \le \theta \le 4\pi$

$$\begin{cases} F_{Ay} = -\dfrac{P(\theta).\pi.D^2}{4} - m_{piston}.g + m_{piston}.r.\dot{\theta}^2.\left(1+\dfrac{\cos\theta}{\sqrt{\delta^2-\sin^2\theta}}\right).\cos\theta + m_{piston}.r.\dot{\theta}^2.\left[\dfrac{\cos^2\theta}{\delta^2-\sin^2\theta} - 1\right]\dfrac{\sin^2\theta}{\sqrt{\delta^2-\sin^2\theta}} \\ F_{By} = -F_{Ay} + m_{bielle}.g - m_{bielle}.r.\dot{\theta}^2.\left[1+\left(1-\dfrac{L_0}{L_1}\right)\dfrac{\cos\theta}{\sqrt{\delta^2-\sin^2\theta}}\right].\cos\theta + m_{bielle}.r.\dot{\theta}^2.\left(1-\dfrac{L_0}{L_1}\right)\left[1-\dfrac{\cos^2\theta}{\delta^2-\sin^2\theta}\right]\dfrac{\sin^2\theta}{\sqrt{\delta^2-\sin^2\theta}} \end{cases}$$

Volume : 4 | Issue : 11 | November 2014 | ISSN - 2249-555X

$$\begin{cases} F_{Bx} = \dfrac{m_{bielle}.L_0.\dot{\theta}^2.\sin\theta}{\delta} - F_{Ax} \\ F_{Ax} = \alpha.m_{bielle}.\dfrac{L_0}{\delta}.\dot{\theta}^2.\sin\theta + \dfrac{L_0}{L_1}.\dfrac{\sin\theta.F_{Ay}}{\delta.\chi} - \alpha.\dfrac{\sin\theta.F_{By}}{\delta.\chi} + \dfrac{\kappa.\dot{\theta}^2.\sin\theta.\left(\dfrac{\cos^2\theta}{\delta^2-\sin^2\theta}-1\right)}{L_1.\delta.\chi^2} \\ \alpha = \left(1-\dfrac{L_0}{L_1}\right) \\ \chi = \sqrt{\delta^2 - \dfrac{\sin^2\theta}{\delta^2}} \end{cases}$$

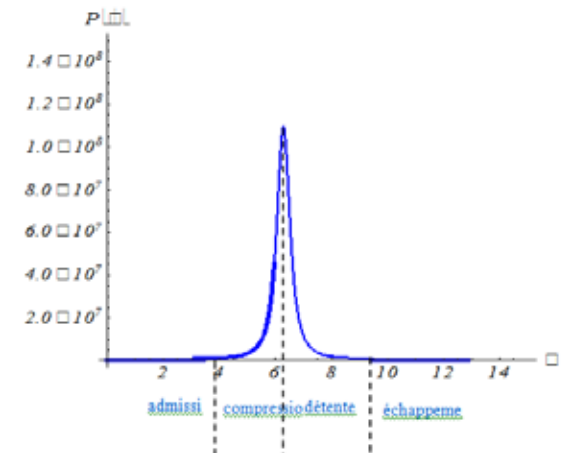

The pressure curve, function of the crankpin angle: the Mathematica code

5- Numerical simulation

2D modeling of the connecting rod by Cast3M.

Using CAST3M: computer code by the method of EF "product under license by CEA"

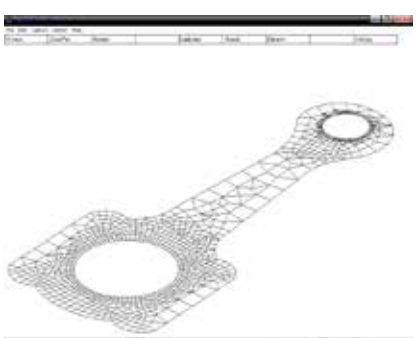

2D mesh by Cast3m

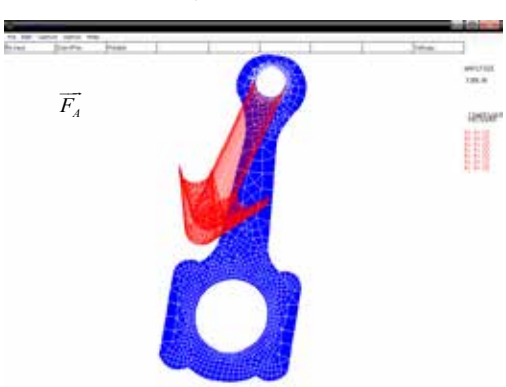

The compressive force at the top end

6- Thermoelastic behavior

Thermal expansion of solids is a general phenomenon, although not very visible, but with serious consequences. The solids expand and contract in the opposite way during their heating and cooling processes.

The combustion of gas "fuel-air" produces heat so the energy to push the piston. If 30% to 50□% energy is converted into work, 70% to 50%□ remains in a state of heat, such excess thermal energy not evacuated, can damage many pieces while in contact with the hot gas and in particular connecting rod of the engine.

In this context we compare the effects of the thermal expansion stress, on the two materials cited above.

Formulation

In the theory of linear thermoelasticity, the convex quadratic thermodynamic potential is given by:

$$\psi = \frac{1}{\rho}\left[\frac{1}{\text{ü}}.\left(\lambda.{\varepsilon_I}^2 + 4.\mu.\varepsilon_{II}\right) - \left(3.\lambda + 2.\mu\right).\alpha.\Theta.\varepsilon_I\right] - \frac{C_\varepsilon}{T_0}.\Theta^2$$

$$\overline{\overline{\sigma}} = \lambda.Tr(\varepsilon)\overline{\overline{1}} + 2.\mu.\overline{\overline{\varepsilon}} - \left(3.\lambda + 2\mu\right)\alpha\Theta\overline{\overline{1}}$$

$$\overline{\overline{\varepsilon}} = \frac{1+\nu}{E}\overline{\overline{\sigma}} - \frac{\nu}{E}Tr(\overline{\overline{\sigma}})\overline{\overline{1}} + \alpha\Theta\overline{\overline{1}}$$

μ and λ: are the two coefficients of Lame

$\overline{\overline{1}}$ unit tensor: second order.

$C_\varepsilon = -T_0\dfrac{\partial^2\psi}{\partial T^2}$ specific heat at constant strain

$$\begin{cases} \sigma_{ij} = \lambda.\varepsilon_{kk}.\delta_{ij} + 2.\mu.\varepsilon_{ij} - (3\lambda + 2.\mu).\alpha.\Theta\delta_{ij} \\ \varepsilon_{ij} = \dfrac{1+\nu}{E}\sigma_{ij} - \dfrac{\nu}{E}.\sigma_{kk}\delta_{ij} + \alpha\Theta\delta_{ij} \end{cases}$$

$$\varepsilon_{ij}\left(\sigma_{ij} = 0, \sigma_{kk} = 0\right) = \alpha\Theta\delta_{ij} = \varepsilon_{ij}\left(\text{thermal}\right)$$

α=f(T) Thermal expansion coefficient;

$\Theta = \Delta T$ temperature variation

An additional linear deformation thermo elastic appears the center distance of the connecting rod and the radius of the crank pin of the crankshaft: $L; L_0; \delta$

By analyzing the two equations of the stress σ_{ij} and the deformation ε_{ij}, we note that the material of the connecting rod expands with the growth of the deformation ε_{ij} ↑ « $+\alpha.\Theta.\delta_{ij}$ ».

Calculations and results

α is a characteristic of the material: factor:

$$\begin{cases} \alpha \approx \dfrac{\gamma_G.\rho.c}{3.E} & \text{equation 1} \\ & \text{factor } \gamma_G \text{ : is the } \textit{Grüneisen constant} \\ \alpha \approx \dfrac{\gamma_G}{100.T_f} & \text{equation 2} \end{cases}$$

γ_G : varies between 0.4 and 4, but usually between 1 and 2 for most solid.

Volume : 4 | Issue : 11 | November 2014 | ISSN - 2249-555X

ρ in kg. m^{-3}, C: is the specific heat $J.kg^{-1}.K^{-1}$, E: Young's modulus (Pa)

$$\begin{cases} E(C-70) \square 213GPa \\ E(PM) \square 199GPa \end{cases}$$

$\rho.c = C_v$ specific heat per volume unit;

It varies little for all solid and therefore E and α are inversely.

$$\begin{cases} \alpha(C-70) \square 21,6.10^{-6} \, m/m^0C \\ E(C-70) \square 213GPa \rangle E(PM) \square 199GPa \\ \alpha(C-70) \square 21,6.10^{-6} \, m/m^0C \langle \alpha(PM) = \frac{E(C-70)}{E(PF)}.\alpha_{C70} \end{cases}$$

$$\alpha_{PM}(\Theta \square 900°C) \square \frac{E(C-70)}{E(PF)}.\alpha_{C70} \square 23,12.10^{-6} m/m.°C$$

Forged to manufacture automobile parts: example
Steel
X60NiMnCr13-5-3
European standards:
AECMA:
- Designation: FE-PA2801
- X60NiMnCr13-5-3
BS : S 131

COMPOSITION
Carbon 0.60
Nickel 11.00
Manganese 5.00
Chromium.....3.00
Molybdenum.....0.40

PHYSICAL PROPERTIES
• Density: 7.9

• Mean coefficient of expansion in m/m.°C:
- between 20°C and 200°C: 20.2 x 10-6
- between 20°C and 400°C: 21.0 x 10-6
- between 20°C and 600°C: 21.3 x 10-6
- between 20°C and 800°C: 21.6 x 10-6

APPLICATIONS
- Fasteners used for assembly of light alloy components working at high temperatures.
- Distribution tubes for valveless engines with pistons and cylinders in light alloys.
- Precombustion chambers fitted to light alloy piston heads for diesel engines.

standard conditions: 25°C

$$\begin{cases} P_1 = P_{atm} \square 1,01325.10^5 Pa \\ V_1 \square 1,917.10^{-3} m^3 \\ V_m \square 2.10^{-5} m^3 \\ L_1 = 15cm \\ r = 38.25mm \\ L(PMH - PMB) = 2.r = 76.5mm \\ \gamma = 1.4 \\ r_0 = \frac{V_{tot}}{V_m} = 1 + \frac{V_d}{V_m} = 18 \\ \Omega = 209.44rad/s = 2000tr/\min(plein.régime) \\ m_{bielle} \square 0.711kg \\ m_{piston} \square 0.422kg \\ L_0 = \frac{2.L_1}{3} \\ D = 75.8cm \\ \delta = \frac{L_1}{r} \end{cases}$$

Full Speed in (taking into account the thermal effect) :

$$\begin{cases} X_f(\square 900°C) = X_i(25°C) + \alpha.\Delta\Theta \\ X = L_1; r; L_0; \delta \end{cases}$$

The comparison is made at maximum pressure which corresponds to the moment of explosion of fuel-air mixture "maximum compression": $\theta = 2.\pi$ rad

$$\begin{cases} P_{25}(2\pi) \square 120MPa = P_{900}(2.\pi) \\ F_{Ay900}(C70) = -5,4150517.10^7 N \\ F_{Ax900}(C70) = F_{Bx900}(C70) = 0N \end{cases}$$

$$\begin{cases} P_{25}(2\pi) \square 120MPa = P_{900}(2.\pi) \\ F_{Ay900}(PF) = -5,415051877.10^7 N \\ F_{Ax900}(PF) = F_{Bx900}(PF) = 0N \end{cases}$$

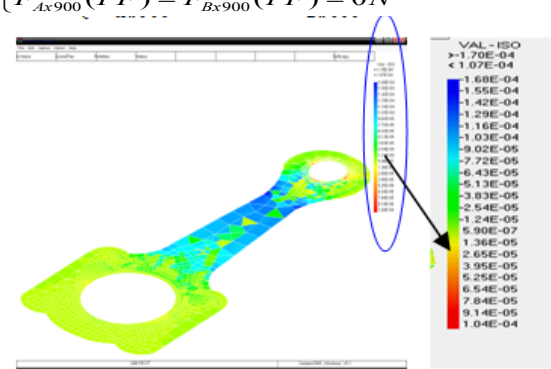

ε_{xx}(PF) mechanical deformation : ambient T°

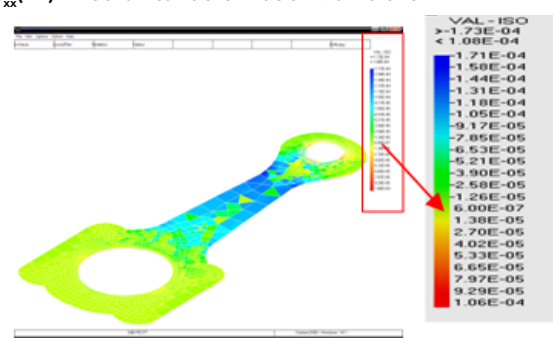

ε (PF) thermomechanical deformation : T° ~900°C

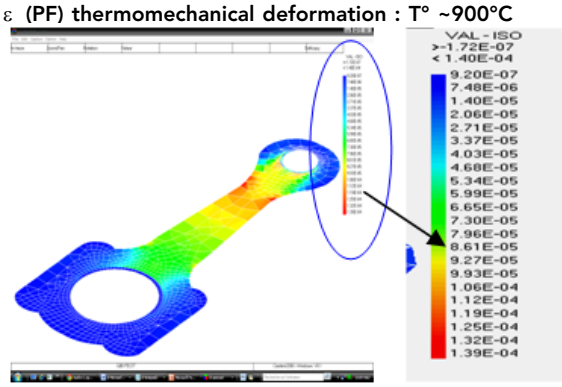

ε_{vM}(PF) thermomechanical deformation T° ~900°C

Volume : 4 | Issue : 11 | November 2014 | ISSN - 2249-555X

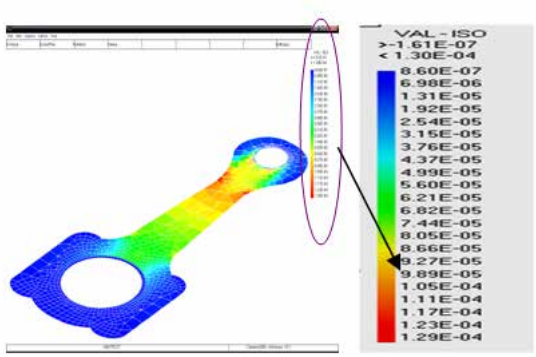

ε_{vM}(C70) thermomechanical deformation T° ~900°C

For ε_{xx} and ε_{yy} deformations, we add

the thermal term $\alpha.\Delta\Theta$.

$$\varepsilon_{ij} = \frac{1+\nu}{E}\sigma_{ij} - \frac{\nu}{E}.\sigma_{kk}\delta_{ij} + \alpha.\Delta\Theta\delta_{ij}$$

$$\varepsilon_{xx}(tot) = \frac{1+\nu}{E}\sigma_{xx} - \frac{\nu}{E}.\sigma_{kk} + \alpha\Delta\Theta$$

$$\varepsilon_{yy}(tot) = \frac{1+\nu}{E}\sigma_{yy} - \frac{\nu}{E}.\sigma_{kk} + \alpha\Delta\Theta$$

It just takes the most stressed areas, the red areas.

- the forged powder /900°C :

a=23,12.10-6m/m0C

$\varepsilon_{xx}.10^5$	-1.26	0.06	1.38	2.70	4.02
ε_{xx}(tot).10^3	20.174	20.231	20.244	20.257	20.270
$\varepsilon_{xx}.10^5$	5.33	6.65	7.97	9.29	10.60
ε_{xx}(tot).10^3	20.283	20.296	20.310	20.324	20.336

- the C70 steel/900°C :

α=21,6.10^{-6}m/m^{0}C

$\varepsilon_{xx}.10^5$	-1.18	0.056	1.29	2.52	3.75
ε_{xx}(tot).10^3	18.89	18.900	18.913	18.93	18.94
$\varepsilon_{xx}.10^5$	4.98	6.22	7.45	8.68	9.91
ε_{xx}(tot).10^3	18.95	18.96	18.97	18.99	19.00

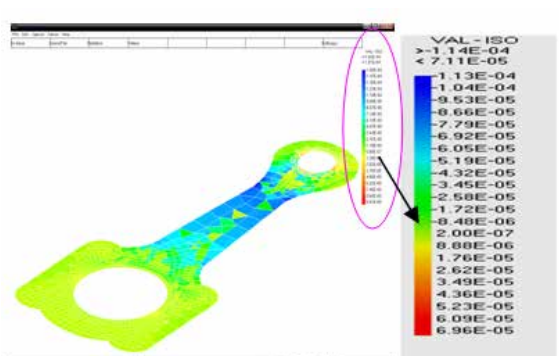

ε_{xx}(C70) thermomechanical deformation ε_{xx}(C70) :T° ~900°C

Same work for the deformation ε_{yy} :

- the forged powder/900°C :

α=23,12.10^{-6}m/m^{0}C

$\varepsilon_{yy}.10^5$	-0.907	0.0214	0.95	1.88	2.81
ε_{yy}(tot).10^3	20.22	20.23	20.24	20.25	20.26
$\varepsilon_{yy}.10^5$	3.74	4.67	5.59	6.52	7.45
ε_{yy}(tot).10^3	20.27	20.28	20.29	20.30	20.31

- the C70 steel/900°C :

α=21,6.10^{-6}m/m^{0}C

$\varepsilon_{yy}.10^5$	-0.85	0.02	0.89	1.76	2.62
ε_{yy}(tot).10^3	18.892	18.900	18.910	18.918	18.926
$\varepsilon_{yy}.10^5$	3.49	4.36	5.23	6.09	6.96
ε_{yy}(tot).10^3	18.935	18.944	18.952	18.961	18.970

Von Mises deformations :

$$\begin{cases} \sigma_{VM} = \frac{1}{\sqrt{2}}.\sqrt{(\sigma_{xx}-\sigma_{yy})^2+(\sigma_{yy}-\sigma_{zz})^2+(\sigma_{zz}-\sigma_{xx})^2+6.(\tau_{xy}{}^2+\tau_{yz}{}^2+\tau_{xz}{}^2)} \\ \varepsilon_{VM} = \frac{\sigma_{VM}}{E} \end{cases}$$

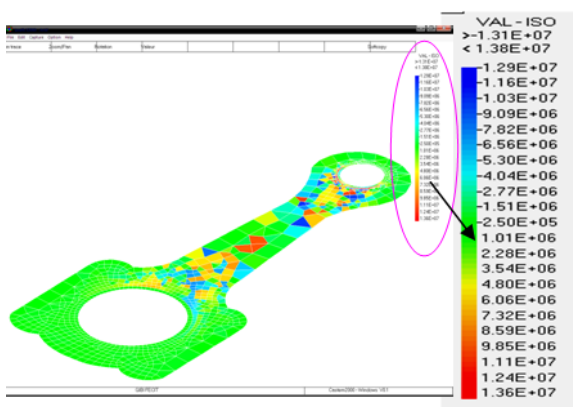

τ_{xy} à Θ~900°C

$$\tau_{xz} = \tau_{yz} = 0; \sigma_{zz} = 0$$

$\sigma_{VM}.10^{-3}$	4.54	8.66	11.53	14.53	17.61
ε_{VM}(PF).10^8	2.28	4.35	5.79	7.30	8.85
ε_{VM}(C70).10^8	2.13	4.07	5.41	6.82	8.27

$\sigma_{VM}.10^{-3}$	20.71	23.86	27.06	30.1
ε_{VM}(PF).10^8	10.41	12.00	13.60	15.13
ε_{VM}(C70).10^8	9.72	11.20	12.70	14.13

Volume : 4 | Issue : 11 | November 2014 | ISSN - 2249-555X

Curves and results:

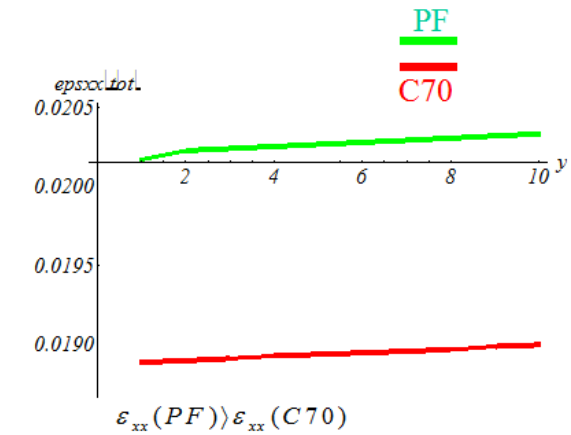

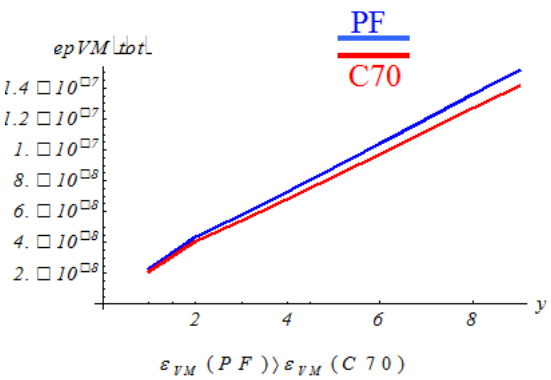

real example

	C70	PMF
e_{xx} max	9,96.10^{-5}	10,60.10^{-5}
e_{xx} (max,tot)	19,00.10^{-3}	20,34.10^{-3}
$\frac{\varepsilon_{xx}(\max, tot)}{\varepsilon_{xx}\max}$	191,73	191,80
e_{yy} max	6,96.10^{-5}	7,45.10^{-5}
e_{yy} (max,tot)	18,97.10^{-3}	20,31.10^{-3}
$\frac{\varepsilon_{yy}(\max, tot)}{\varepsilon_{yy}\max}$	272,56	272,62

Summary results

7- Conclusion

According to the study that was conducted, we observe that the mechanical deformations ε_{xx} and ε_{yy} multiplied almost respectively 200 and 300 times when the temperature of the combustion chamber attained 900 ° C.

Under the effect of thermal expansion, although

ε_{ii} (C70)≅ ε_{ii} (PM), the two structures of the two materials undergo large deformations compared to the normal state.

The effect of excessive heat added to a low efficiency in cases of fatigue the engine and any inadequate lubrication, are sufficient factors to cause rupture such an important piece that the connecting rod.

Hence the attention, very special to give quality structure of these materials for the production of auto parts in order to predict a catastrophic impact the functioning of thermal engine block in its entirety.

REFERENCE

1. Cetin Morris Sonsino, Dynamic Properties of PM Materials,PM2001, Concepts and Required Materials Data for Fatigue Design of PM Components, Fraunhofer-institute for Stmcturel Durability (LBF), Barbringstr 47, D-64289 Darmstadt, Germany | | 2. Imahashi, K., C. Tsumuki, and I. Nagare, Development of Powder-Forged Connecting Rods, Society of Automotive Engineers, Society of Automotive Engineers, 1984. | | 3. Heat Treating;1991;Volume 4 of the ASM Handbook. The ASM Handbook Committee. | | 4. Powder Metal Technologies and Applications; 1998; Volume of ASM Handbook. The ASM Handbook Committee. | | 5. Pravardhan S. Shenoy, Dynamic Load Analysis and Optimization of Connecting Rod, The University of Toledo | May 2004 | | 6. Adila Afzal and Pravardhan Shenoy,Graduate Research Assistants and | Ali Fatemi, Professor The University of Toledo | | 7. Pravardhan S. Shenoy et Ali Fatemi Université de Toledo : Connecting Rod Optimization for Weight and Cost Reduction 2005-01-0987 | | 8. Lemaitre, C., P. Dierickx, and G. Bittes, Steels For High Performance Diesel Engines, 2006 New Developments in Long and Forged Products Proceedings, 2006. | | 9. Lee, C.S., Y.S. Ko, S.H. Kim, H. Park, and J.D. Lim, Development of High Strength, Fracture Split Steel Connecting Rods. Society of Automotive Engineers, 2007. 07M-343. | | 10. Kato, S., T. Kano, M. hobo, Y. Yamada, T. Miyazawa, and Y. Okada, Development of Microalloyed Steel for Fracture Split Connecting Rod. Society of Automotive Engineers, 2007. 07M-385. | 11. Powder metal forged and C-70 Steel forged. Fatigue analysis of connecting rod |